A Novel Interlaced Sampling Scheme for Multi-Shell q-space Magnetic Resonance Microscopy

S. Portnoy[1], W. Ye[2], A. Entezari[2], S. J. Blackband[1,3], and B. C. Vemuri[2]
[1]Department of Neuroscience, University of Florida, Gainesville, Florida, United States, [2]CISE department, University of Florida, Gainesville, Florida, United States, [3]National High Magnetic Field Laboratory, Tallahassee, Florida, United States

INTRODUCTION: A major goal of diffusion MRI is the reconstruction of the 3D diffusion propagator, *P(**r**)*, which specifies the probability for a water molecule to displace by a vector, ***r***, given a diffusion time, Δ. Since molecular motion in biological systems is restricted by interactions with tissue components such as cell membranes, macromolecules and fibers, *P(**r**)* provides useful information about tissue structure and connectivity [1].

The 3D diffusion propagator is obtained using q-space MRI techniques, which rely on the Fourier relationship between *P(**r**)* and the diffusion-based echo attenuation, *E(**q**)* [2]. *P(**r**)* is calculated from the 3D IFFT of *E(**q**)* data, which is sampled uniformly over 3D **q**-space . This requires a large number of diffusion experiments, which makes this approach very time consuming. It is therefore important to employ an efficient **q**-space sampling scheme which provides the most accurate reconstruction of the diffusion propagator. In practice, the most widely used scheme is to take a sample at the origin (**q**=0) together with uniformly distributed samples on one or more spherical shells [3, 4].

In this work, we propose a novel interlaced multi-shell sampling scheme. Unlike standard schemes, which have the same directional distribution of samples on each shell, this technique uses two different polyhedra, the icosidodecahedron and rhombic triacontahedron, to determine the sample distributions on odd and even shells. Results show that, even with slightly fewer samples than the typical multi-shell scheme, the interlaced scheme has higher reconstruction accuracy. Moreover, the accuracy can be further improved by using the interlaced scheme in combination with a body-centered-cubic (BCC) **q**-space sampling lattice [5].

METHODS

Sampling Schemes: In the interlaced sampling scheme, we used the vertex directions of the rhombic triacontahedron (32 vertices) and its dual, the icosidodecahedron (30 vertices), to determine the sampling directions on odd and even **q**-shells, respectively. Due to the symmetry of the diffusion signal (i.e. S(**q**)= S(-**q**)), only half of the sampling directions are necessary. For comparison, we also simulated and acquired data with a standard sampling scheme, where the vertices of the rhombic triacontahedron defined the sampling directions for all shells.

Simulations: To test the effectiveness of the interlaced scheme, we generated a synthetic dataset from a mixture of two oriented Gaussian functions to simulate the diffusion signal from a pair of crossing fibers. One of the Gaussian components was fixed, while the second component was varied to make a fiber crossing angle of 20-60 degrees with a 5 degree step size. Samples of the **q**-space signal were taken according to both sampling schemes on 7 spherical shells uniformly distributed between 0 and $q_{max}= 0.5\sqrt{1/20}$ m^{-1}. The total number of samples was 193 for the standard scheme and 187 for the interlaced scheme.

Data Acquisition: We acquired real **q**-space Magnetic Resonance Microscopy (MRM) data on a coronal mouse brain section at the level of the superior colliculus. This region was chosen based on its known abundance of in-plane crossing fibers [6]. MRM was performed on a 14.1 Tesla Bruker Biospin imaging spectrometer, using a conventional diffusion weighted spin echo pulse sequence. Acquisition parameters included: slice thickness=0.3 mm, 1.2x1.2 cm^2 field-of-view, 192 x 192 data matrix, 62.5 μm in-plane resolution, diffusion time, Δ=12 msec, and diffusion gradient duration, δ=1 msec. Data was acquired on 5 spherical shells uniformly distributed between **q**=0 and $\mathbf{q}_{max}$=81 mm^{-1}. The total number of samples was 65 for the standard scheme and 63 for the interlaced scheme.

Reconstruction of *P(r**)*:** The reconstruction of *P(**r**)* was performed by interpolation of the spherically distributed **q**-space samples onto a Cartesian and body-centered-cubic (BCC) grid, followed by inverse Fourier transformation. The BCC grid was used because it is the 3D lattice with the highest sampling efficiency. The Fourier transform of the BCC grid is the face-centered cubic (FCC) grid, which corresponds to the densest sphere packing in space. BCC sampling in **q**-space has been shown to provide greater resolution of *P(**r**)* and minimize distortions due to aliasing [5].

RESULTS & DISCUSSION: The reconstructions of the diffusion propagator from the synthetic **q**-space datasets is shown in Figure 1. For a quantitative comparison of reconstruction accuracy, the mean square error (MSE) of the reconstructed *P(**r**)* relative to the simulated *P(**r**)* was calculated. The results for a selection of crossing angles are summarized in Table 1. Reconstructions obtained from the interlaced scheme are sharper and more accurate than those obtained from the standard scheme. As shown in the bottom rows of Figure 1 and Table 1, even greater accuracy in the reconstruction of *P(**r**)* can be obtained using a BCC grid, owing to reduced distortion due to aliasing [5].

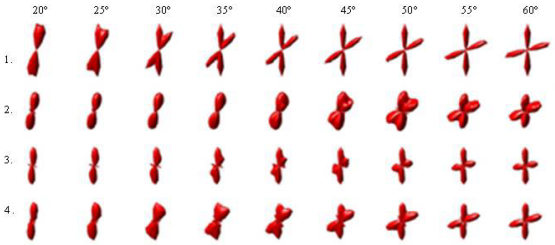

Figure 1: Reconstruction of simulated *P(**r**)* using different sampling/reconstruction schemes. Row 1: original simulated structure. Row 2: reconstruction using standard scheme interpolated onto a Cartesian grid. Row 3: reconstruction using interlaced scheme with Cartesian grid. Row 4: reconstruction with interlaced scheme and BCC grid.

Table 1: Mean square error of simulated data reconstruction

Scheme	20°	30°	40°	50°	60°
Standard/Cartesian	12.93%	13.07%	13.05%	12.69%	12.10%
Interlaced/Cartesian	6.04%	6.67%	5.20%	5.44%	5.58%
Interlaced/BCC	4.54%	4.28%	3.45%	4.62%	4.19%

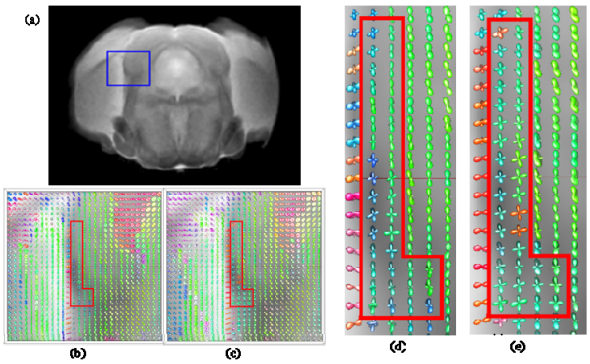

Figure 2: Reconstruction of real **q**-space data. (a) **q**=0 image. (b), (c) reconstructed *P(**r**)* maps for the ROI indicated by the blue box – (b) =standard scheme with Cartesian grid, (c) =interlaced scheme with BCC grid. (d),(e) zoomed in versions of (b) and (c). The red box shows the area where the interlaced/BCC technique recovered crossings, while the standard/Cartesian method failed.

Close-ups of the reconstructed diffusion propagator maps in a region of interest on the acquired mouse brain data are shown in Figure 2 (d), (e). The reconstruction obtained from the standard scheme interpolated onto a Cartesian grid is shown in (d) and the reconstruction obtained from the interlaced scheme interpolated onto a BCC grid is shown in (e). As demonstrated by the red box, the combination of interlaced sampling and BCC gridding recovers many crossings, while the standard scheme fails.

CONCLUSION: This work introduces an interlaced multi-shell q-space sampling technique for the reconstruction of the 3D diffusion propagator. Comparison with the standard multi-shell scheme on simulated and acquired MR data shows greater accuracy in the reconstruction of *P(**r**)*, even with marginally fewer **q**-space samples. The accuracy of the interlaced method is improved even further by interpolation of the **q**-space samples onto a body-centered-cubic sampling grid. When used in combination, interlaced sampling and BCC interpolation provide a significant improvement in our ability to resolve the complex fiber architectures within biological tissues.

REFERENCES: [1]Le Bihan, D. et al. 2006. JMRI 24: 478-488. [2]Callaghan, P.T. *Principles of Nuclear Magnetic Resonance Microscopy*. Clarendon Press, Oxford, 1991. [3] Tuch, D. 2004. MRM 52: 1358-1372. [4] Descoteaux, M. et al. 2010. Med. Image Anal. Epub ahead of print. [5] Ye, W. et al. 2010. Proc IEEE Int Symp Biomed Imaging 788-791. [6]Leergaard, T et al. 2010. PLoS ONE 5:e8595.